Ultrasound Indications in Implant Related and Other Oral Surgery

7

Hsun-Liang (Albert) Chan and Oliver D. Kripfgans

7.1 Introduction

The number of dental implant procedures to replace missing dentition is rapidly increasing and has become the standard of care owing to the high survival rate [1, 2]. Successful implant treatment requires prudent evaluation of the surgical site and comprehensive treatment planning, including use of imaging. Features of an ideal imaging modality include: accurate, versatile, no harm, user-friendly, and cost efficiency, etc. [3]. Currently, two-dimensional (2D) imaging modalities, e.g. intraoral radiographs and panoramic films, are the most commonly used. Nevertheless, image magnification/distortion and the lack of cross-sectional information, etc. are among the major disadvantages [4]. The use of Cone-Beam Computed Tomography (CBCT) is on a rise in recent years [5]. The American Academy of Oral and Maxillofacial Radiology (AAOMR) recommends that evaluation of a potential implant site should include cross-sectional imaging [6]. As useful as CBCT can be, certain disadvantages limit its routine use, i.e. inferior soft tissue contrast, higher cost, higher radiation exposure, and suboptimal imaging quality from interfering artifacts created by metal objects [7, 8]. In medicine, ultrasound always precedes use of CT scans. A systematic review [9] was conducted by our research group to understand the current status of dental ultrasonography research and its potential for clinical use in implant therapy. Table 7.1 summarizes the search results categorized by the

H.-L. (Albert) Chan
Department of Periodontics and Oral Medicine, School of Dentistry, University of Michigan, Ann Arbor, MI, USA
e-mail: hlchan@umich.edu

O. D. Kripfgans (✉)
Department of Radiology, Medical School, University of Michigan, Ann Arbor, MI, USA
e-mail: greentom@umich.edu

H.-L. (Albert) Chan, O. D. Kripfgans (eds.), *Dental Ultrasound in Periodontology and Implantology*, https://doi.org/10.1007/978-3-030-51288-0_7

Table 7.1 Potential clinical indications of ultrasonography for different phases of implant therapy [5] (modified from Bhaskar et al. [9] with permission)

Treatment phase	Potential indications
Planning phase	• Evaluate soft and hard tissue phenotype • Identify vital structures • Evaluate ridge width • Indicate bone density
Surgical phase	• Evaluate cortical bone • Identify vital structures • Evaluate drill bit-bone boundary distances
Follow-up phase	• Indicate primary stability (Chap. 10) • Evaluate marginal bone level around implants (Chap. 8) • Indicate implant-bone stability (Chap. 10)

implant treatment timing, i.e. treatment planning, intraoperative, and postoperative phases.

Table 7.2 summarizes the research and development status of ultrasound imaging, ranging from benchtop studies, preclinical and clinical studies for all possible implant related indications. This review demonstrated a continuous interest in ultrasound imaging in dental research, reflected by published studies proposing numerous indications with which ultrasound can be applied during the three phases of implant treatment. This chapter will focus on indications during pre-surgical treatment planning and during the surgery. Evaluation of marginal bone level after implants are placed will be discussed in detail in Chap. 8. Chapter 10 will specifically focus on ultrasound-based assessment of implant-bone stability. Wound healing evaluated by ultrasound will be discussed in Chap. 9. Peri-implant structure evaluation using ultrasound will be described in Chap. 6.

7.2 Pre-Surgical Treatment Planning

7.2.1 Tissue Phenotype Evaluation

Soft tissue phenotype is relevant to soft tissue strength for resisting mechanical trauma, tissue recession tendency, implant esthetics, and peri-implant bone remodeling, etc. It is in part determined by soft tissue thickness. Several authors investigated the accuracy of using ultrasound to measure soft tissue thickness [10–12, 14]. These validation studies used either human cadavers or porcine cadavers, with ultrasound frequencies at 5, 10, and 16.1 MHz. The mean difference between ultrasound and direct soft tissue thickness readings was 0.13 mm [14], 0.2 mm [10], 0.3 mm [12], and 0.5 mm [11]. In the last two studies, the measured tissue thickness was approximately 5 mm; therefore, the measurement deviation was approximately 10%. One study [14] found a strong correlation ($r = 0.89$) between ultrasound and direct measurements. Two studies [13, 14] applied ultrasound to measure soft

Table 7.2 Summary of the studies classified by the main indications and study designs (modified from Bhasker et al. [9] with permission)

Indication category	Specific parameter to measure	First author (year)	Study design Preclinical/ simulation	Clinical human
Soft tissue evaluation	Tissue thickness	Traxler [10]	V	
		Culjat [11]	V	
		Culjat [12]	V	
		De Bruyckere [13]		V
		Eghbali [14]	V	V
		Chan [14]	V	
		Tattan [15]		V
Hard tissue evaluation	Ridge Width	Traxler [16]	V	
	Peri-implant bone level	Bertram [17]		V
		Chan [14]	V	
	Bone density	Klein [18]		V
		Kammeler [19]	V	
	Crestal bone level	Salmon [20]		V
	Cortical bone thickness	Degen [21]	V	
	Crestal bone level and thickness	Chan [22]	V	
		Tattan [15]		V
Vital structure evaluation	Sublingual a.	Lustig [23]		V
	Inferior alveolar canal & maxillary sinus	Machtei [24]		V
	Bone boundaries	Rosenberg [25]	V	V
	Inferior alveolar canal	Zigdon-Giladi [26]		V
	Greater palatine foreman, mental foramen and lingual n.	Chan [27]	V	
	Lingual structures	Barootchi [28]	V	V
Implant stability evaluation	Transmission sound velocity	Veltri [29]	V	
		Kumar [30]	V	
	Transmission sound energy	Ossi [31]	V	
		Ossi [32]	V	
		Mathieu [33]	V	
		Mathieu [34]	V	
	Reflection sound amplitude pattern	Vayron [35]	V	
		Vayron [36]	V	
		Mathieu [37]	V	
		Vayron [38]	V	
		Vayron [39]	V	

tissue dimensional changes after a grafting procedure around implants in humans. A reduction of approximately 0.1 mm in soft tissue thickness was found at 1 year. These studies demonstrate the accuracy of ultrasound in estimating oral soft tissue thickness.

Hard tissue phenotype, i.e. crestal bone thickness, is another important parameter because it is related to the amount of ridge resorption after tooth extraction, peri-implant bone volume, and implant success. A descriptive study [20] suggested the crestal bone level was detectable in at least 90% of the studied sites (162 sites from three patients) on ultrasound images obtained by using a 25 MHz probe and a newly designed ultrasound system. Our group showed an accurate estimation of crestal bone height and thickness on human cadavers by using a commercially available ultrasound scanner (ZS3, Mindray) [27]. The correlations of the ultrasound readings to CBCT and direct measures were between 0.78 and 0.88, respectively. The mean absolute differences in crestal bone height and thickness between ultrasound and CBCT were 0.09 mm (95% CI: −1.20–1.00 mm) and 0.03 mm (95% CI: −0.48–0.54 mm), respectively. Figure 7.1 showed evaluation of tissue phenotype with ultrasound. In addition to soft tissue thickness, B-mode ultrasound imaging can provide useful anatomical information about the muscle attachment level, tissue characteristics (pixel brightness) that may be related to tissue elasticity, supracrestal soft tissue height, and mucosal margin angle, etc. Figure 7.2 illustrated ultrasound

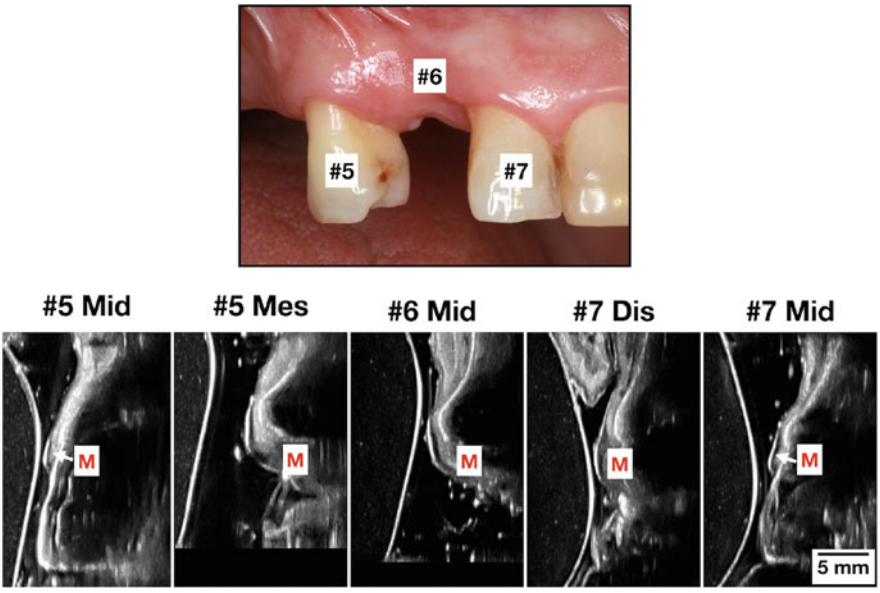

Fig. 7.1 The periodontal tissue around teeth #5 and #7 and edentulous tissue dimensions around tooth #6 location were evaluated with ultrasound. The mucosal (M) thickness, the supracrestal tissue dimension (including sulcus), and the interdental papilla height, etc. can be measured from these images

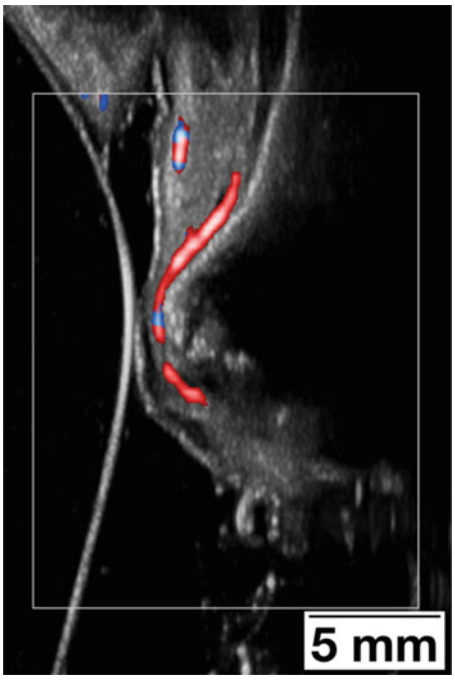

Fig. 7.2 A color-flow image of periodontal tissues. In addition to soft tissue dimensions, this type of ultrasound image can evaluate the blood flow, which could be very valuable for periodontal disease diagnosis and wound healing evaluation

can quantify blood flow in periodontal tissue that could be of a great diagnostic value in periodontal disease diagnostics and wound healing evaluation. The vessel shown immediately adjacent to the alveolar bone is a supraperiosteal vessel with a size of 100–200μ.

7.2.2 Jawbone Density

Jawbone density has also been evaluated by ultrasound [18]. A 1.2 MHz ultrasound scanner (DBMSonic 1200 instrument, IGEA, Carpi, Italy) was used to measure the ultrasound transmission velocity (UTV) values at different anatomical jaw locations on 108 patients. It was composed of 2 transducers, which were placed on the facial and lingual/palatal side of the jaw. The device recorded the period of the fastest signal conducted through the bone as an indicator of bone density. Similar technology had been applied to orthopedic medicine. Significantly higher UTV was found in maxillary anterior and mandibular posterior regions than in maxillary posterior regions. It was concluded that assessment of alveolar ridge using UTV might offer the possibility to identify bone quality before implant surgery or to monitor bone healing after augmentation procedures. A subsequent study using the same device correlated UTV to bone density measured from histomorphometry, CBCT, and micro-CT [40]. Bone quality of ex vivo cortical, cancellous, and mixed bone blocks were measured and compared. Amplitude-dependent UTV values were

obtained. UTV values were 1945.17, 1266.9, and 1472.2 m/s for cortical, cancellous, and mixed samples. There was a high correlation ($r > 0.9$) between UTV values and those from histomorphometry and radiography. Cortical bone thickness, another important clinical parameter, was determined with a combination of low (5 MHz) and high (50 MHz) frequency ultrasound set up [21]. The cortical bone thickness was measured at specific sites around implants using ultrasound, CBCT, and stereomicroscopy. Ultrasound and CBCT measurements deviated from the true bone thickness by approximately 10%. The authors concluded that ultrasound has a high potential to supplement CBCT in measurement of cortical bone thickness.

7.2.3 Edentulous Ridge Width

Ridge width is among the most important clinical parameters for implant therapy. It primarily determines the implant diameter and if a bone augmentation procedure is required. Residual ridge width was measured with ultrasound on 11 sites from 4 patients and compared to open bone measurements [16]. An ultrasound device with a 10 MHz mechanical sector and linear transducers was used. This study concluded that the ultrasound measurement produced nearly the same data as ridge mapping. Figure 7.3 illustrated the accuracy of ultrasound in imaging crestal bone ridge width. It can also image the integrity of cortical bone. With normal bone ridge, the ultrasound image of the crestal bone is a continuous and hyperechoic line. When there is soft tissue invagination or impaired bone healing, the cortical bone surface shows irregularity or discontinuous and less hyperechoic. Ultrasound can potentially become a screen tool for assessing ridge width and cortical bone quality before implant surgery.

7.2.4 Maxillary Palate Anatomy

The maxillary nerve (CNV2), the 2nd branch of the trigeminal nerve, innervates the mid-third of the face. After leaving the trigeminal ganglion, the nerve passes through the foramen rotundum before leaving the skull and gives rise to many sensory branches. Some branches that are relevant to dentistry are (1) superior alveolar nerve, (2) infraorbital nerve, (3) greater and lesser palatine nerves and nasopalatine nerve. While infiltration of anesthetic injections is usually sufficient for short surgical procedures in the maxilla, advanced procedures, e.g. quadrant osseous periodontal flap surgery, bone regeneration, lateral sinus augmentation, and full arch rehabilitation, may require block anesthesia of CNV2. Intraorally, anesthesia of CNV2 can be achieved from the greater palatine canal (GPC), through which the greater palatine nerve travel after it is branched off from the maxillary nerve. Therefore, it is important to identify the canal and its opening in the oral cavity, the greater palatine foramen (GPF). In the literature, landmarks, e.g. molar teeth, midline maxillary suture, the posterior border of the hard palate, etc., have been used but are not satisfactory to locate the GPF [41]. In general, it is located at

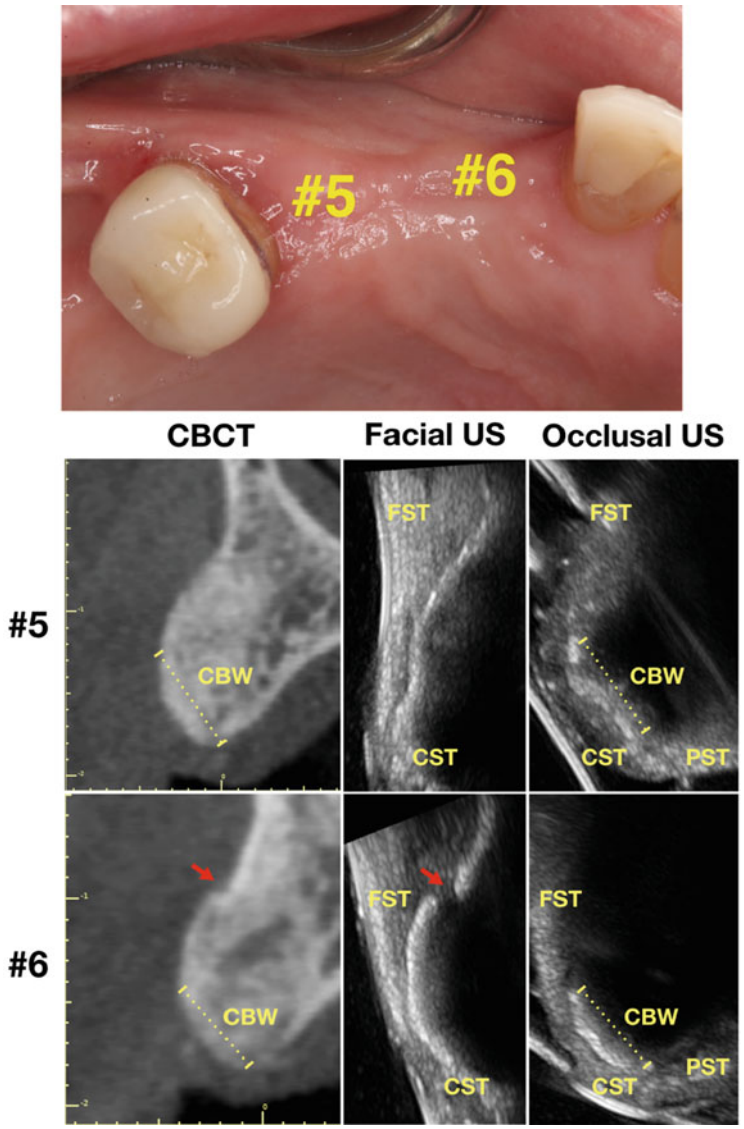

Fig. 7.3 Top, A clinical photo of teeth #5 and #6 planned for implant surgery. Bottom, Facial and occlusal ultrasound scans, with CBCT as a reference, to show crestal bone width (CBW) measures. The red arrow indicates a step between native and newly formed bone, which is also shown on the ultrasound image. FST: facial soft tissue; CST: crestal soft tissue; PST: palatal soft tissue

the junction of the hard palate process and the maxillary alveolar process, mesial or opposite to the 3rd molar; however, the exact location varies from individual to individual [42]. Therefore, imaging-guided block anesthesia of the maxillary

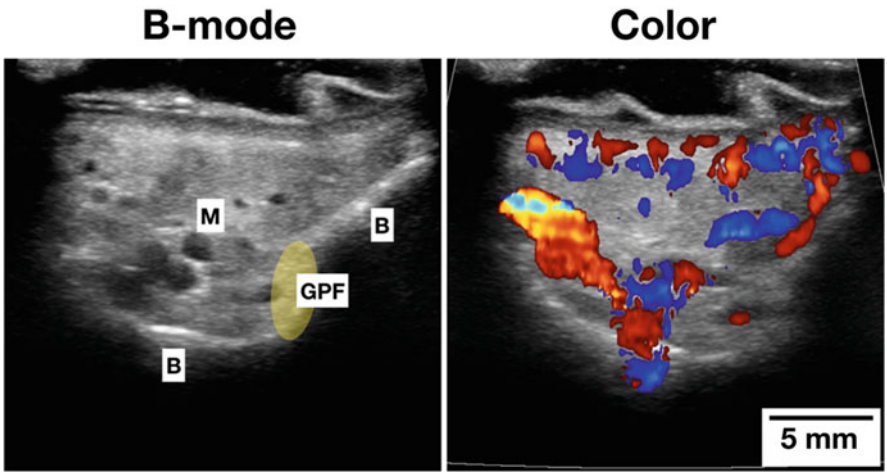

Fig. 7.4 B-mode and color-flow images of the greater palatine foramen (GPF). The bright line is the maxillary bone (B). The discontinuous line is the GPF location. The Color flow shows the greater palatine vessels in the region. M: mucosa

nerve is needed. Ultrasound can provide GPF location in real time during injection. Figure 7.4 illustrates an image of the GPF in a live human. The white line is the maxillary bone surface. Discontinuity of the white line indicates the foramen. B-mode may already show the foramen. Sometimes the Color mode can be used to confirm its location by showing the course of the blood flow in the greater palatine artery/vein, which travel together with the nerve in the canal.

Once the canal is identified, a standard dental long needle (32 mm long) is inserted almost to the end and 1.8 cc of lidocaine is administered slowly after aspiration. CBCT can be helpful to gauge the length of the canal. On average the canal length is 32 mm. Injection beyond the canal into the pterygopalatine fossa and even into the cranium will lead to serious complications, e.g. direct nerve damage, hematoma, diplopia (double vision), transient ophthalmoplegia, ptosis, temporary blindness, and unconsciousness, etc. Therefore, it is important not to pass the needle over the total length of the canal.

Periodontal/peri-implant plastic surgery to cover exposed roots/implants and correct other soft tissue deficiencies is a common procedure. Autogenous tissue harvested from the palate is still the gold standard for this type of procedures. Therefore, knowledge about the quality and quantity of the palatal mucosa is key. The area adjacent to the premolars is a common donor site. Ultrasound can accurately measure tissue thickness and vascularity so the surgeon will know at chairside if there is adequate soft tissue thickness for harvest or allograft will have to be used. Knowing the vascularity can help the surgeon to expect the bleeding tendency, which often time complicates the surgery (Fig. 7.5).

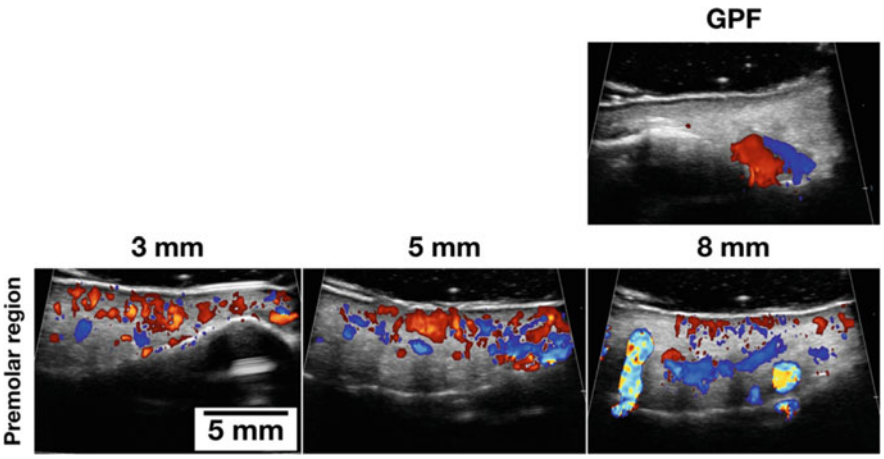

Fig. 7.5 The vessels in the GPF (top) and the palate at the premolar region at 3, 5, and 8 mm from the cementoenamel junction (CEJ). The palatal thickness and vascularization can be evaluated and measured before the grafting harvesting surgery

Box 1
Ultrasonography can image the greater palatine canal, which is a gateway for block anesthesia of the maxillary nerve. Anesthesia of this nerve is often needed for major surgical procedures, e.g. lateral window sinus augmentation.

7.2.5 Mandibular Lingual Anatomy

The lingual nerve is a branch of the mandibular nerve, the 3rd branch of the trigeminal nerve. This nerve provides sensory innervation to the mucous membranes of the anterior two-thirds of the tongue and the lingual tissues. It also accompanies chorda tympani nerve to provide taste sensation of the anterior two-thirds of the tongue. After branching off from the mandibular nerve, it travels in the pterygomandibular space along with the inferior alveolar nerve (IAN). While the IAN goes into the mandible through the mandibular foramen, the lingual nerve stays in soft tissue, running beyond the anterior edge of the medial pterygoid muscle and descend toward the distal side of the third molar. It is located at a mean 3 mm apical to the osseous crest and 2 mm horizontally from the lingual cortical plate in the third molar area [43]. Nevertheless, the nerve may be situated at or above the crest of bone in 15–20% cases [44]. Furthermore, 22% of the time the nerve may contact the lingual cortical plate [43]. Once passing the 3rd molar, it travels mesially, apically, and medially toward the tongue. Seventy-five percent of lingual nerves turned toward the tongue at first and second molar region. The vertical distance

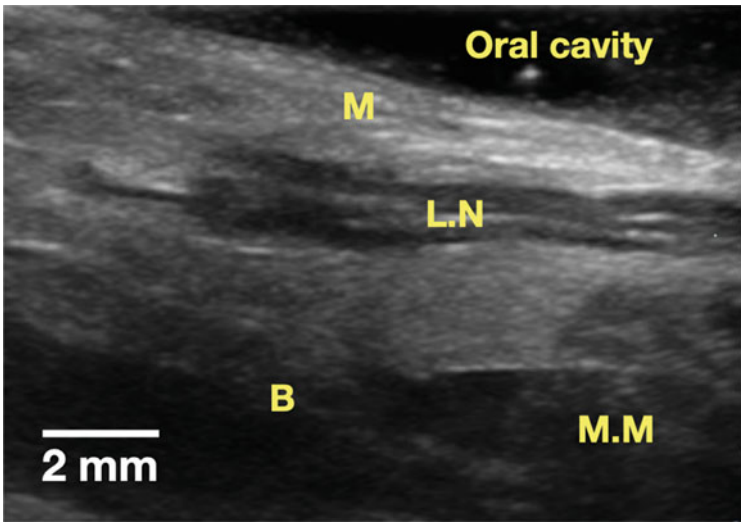

Fig. 7.6 Illustration of the lingual nerve (L.N) and the adjacent structures. M: mucosa; M.M: mylohyoid muscle; B: Lingual plate of the mandible

between the nerve and the cementoenamel junction (CEJ) of the second molar, first molar, and the second premolar was 9.6, 13, and 14.8 mm, respectively [45]. Because its superficial location in general in the 3rd molar region, precaution has to be exercised when performing a flap surgery in this area, e.g. 3rd molar extraction, bone augmentation surgery, and periodontal surgery. A 0.6–2% incidence of lingual nerve injury has been reported following third molar extraction [46–50]. One way to avoid traumatizing this nerve is to know its location. Ultrasound may be the most ideal imaging modality for this nerve because it cannot be seen on radiographs. Our group published a proof-of-principle study [45] and a subsequent study showing ultrasound can image the lingual nerve [28]. Figure 7.6 illustrates the lingual nerve. The nerve is shown as a hypoechoic linear structure with hyperechoic streaks, a character of many other nerves in the body composed of fascicles (a group of nerve fibers in the main nerve).

Another clinical indication for locating the lingual nerve is for its block anesthesia. The most common target for local anesthesia of the lingual nerve is the pterygomandibular space. Once the inferior alveolar nerve is anesthetized, the long needle is withdrawn half way where the lingual nerve is anesthetized. However, inadequate anesthesia of the lingual nerve is common because of the unreliable landmarks. Exclusive lingual nerve block at the 3rd molar region can be an effective alternative because of the following advantages: (1) greater success rate due to easier and closer access, (2) aspiration is not required because of no major vessels in this area, and (3) less chance of post-injection trismus (limited mouth opening). Blind injection in the lingual mucosa of the 3rd molar may already have profound anesthesia of the lingual nerve. Visualization of the nerve with ultrasound can

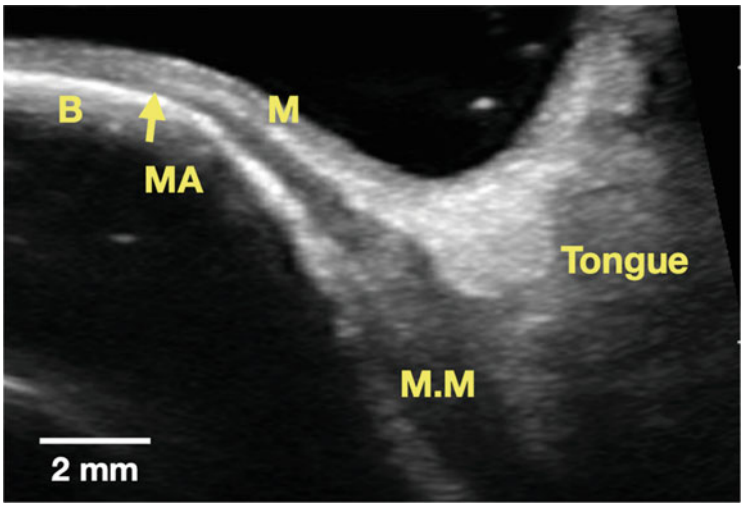

Fig. 7.7 Ultrasound illustration of the lingual structures, including the lingual plate of the mandible (B), the mucosa (M), the mylohyoid muscle (M.M), and the attachment of the mylohyoid muscle (MA)

improve clinician confidence, increase anesthesia success rate and working time, and reduce injection quantity. Moreover, ultrasound can be a learning tool for dental students to practice lingual nerve anesthesia.

Anatomy of the mandibular lingual region has becoming more important because of the popularity of performing bone regeneration for implant placement in this region. Lingual flap releasing requires detachment of the lingual mucosa from the underlying mylohyoid muscle. Knowledge of relevant anatomy besides the above mentioned lingual nerve, i.e. the lingual mucosa thickness, sublingual salivary glands, and mylohyoid muscle attachment is key to successful lingual flap management. Our recent ultrasound cadaver study showed that the mean mucosal thickness is 1.45±0.5 and 1.54±0.5 mm, measured at 5 and 10 mm from the mucosal margin, respectively [28]. Histology showed similar dimension, 1.40±0.51 and 1.37±0.50 mm, without statistical significance. The mean mylohyoid muscle dimension is 2.32±0.56 and 2.47±0.57 mm, respectively at 5 and 10 mm from the muscle attachment. Again, similar dimension was measured on histology, without statistical significance (Fig. 7.7). Regarding the lingual nerve dimension, the cross-sectional diameter was 2.38 ± 0.44 and 2.5 ± 0.35 mm at the 3rd molar and retromolar sites, compared to 2.43 ± 0.42 and 2.54 ± 0.34 mm on the histology, respectively, without statistical significance.

7.2.6 Mental Foramen Evaluation

The mental foramen is the pathway for the mental nerve, the terminal branch of the inferior nerve, and its accompanying vascular bundles. There are three nervous branches emerging from this foramen, providing sensations to the skin, lower lip, gingiva, and mucous membrane mesial to the second premolar to the midline. According to our retrospective cone-beam computed tomography study [51], the mental foramen is located either below the apex of second premolar or between the first and second premolars in 82% of the cases. Its vertical location is halfway between the CEJ and the lower border of the mandible with a range from 13.3 to 23.6 mm from the CEJ and between 12.2 and 20.7 mm from the inferior border of the mandible. Injury to this important nerve can result in temporary or permanent paresthesia, with an incidence rate of up to 7% of cases [52–54]. Therefore, knowledge of the mental foramen location is necessary when performing surgery in this area. Before and during a surgery in this area, ultrasound can provide mental foramen location in real time; therefore, it will be of great value in minimally invasive procedures, e.g. flapless implant surgery. Our group demonstrates ultrasound can image mental foramen in a cadaver study [22]. Figure 7.8 shows features of mental foramen on ultrasound image in a live human.

7.2.7 Other Anatomical Structures

The sublingual artery is another important structure in the anterior lingual mandible that can be identified by ultrasound [23]. Although rare, injury of this vessel can result in massive hemorrhage in the sublingual and submandibular spaces, which in turn can cause fatal airway obstruction. The diameter, direction of blood flow, and blood volume were evaluated in 20 subjects by using a 10-MHz superficial transducer. In all subjects, blood flow was identified and directed into the bone. The average diameter of the artery was 1.41($\pm$0.34 mm) and the average blood flow 2.92 $\pm$ 3.19 mL/min. The ultrasound/Doppler is a reliable tool to visualize and measure the blood supply to the anterior mandible.

7.2.8 Intra-Surgical Evaluation

During osteotomy ultrasound waves can be sent into bone through the osteotomy site. Sound impedance differences between cancellous bone and more dense cortical bone surrounding important structures could then locate these structures, e.g. the inferior alveolar nerve (IAN) and the maxillary sinus. A novel ultrasound device was used to identify IAN and the maxillary sinus intraoperatively on 14 patients [24]. The ultrasound readings were compared to measurements made from panoramic radiographs. The overall differences between the ultrasound and radiographic measurements were minor (0.4 mm), with positive correlation ($r = 0.57$). After

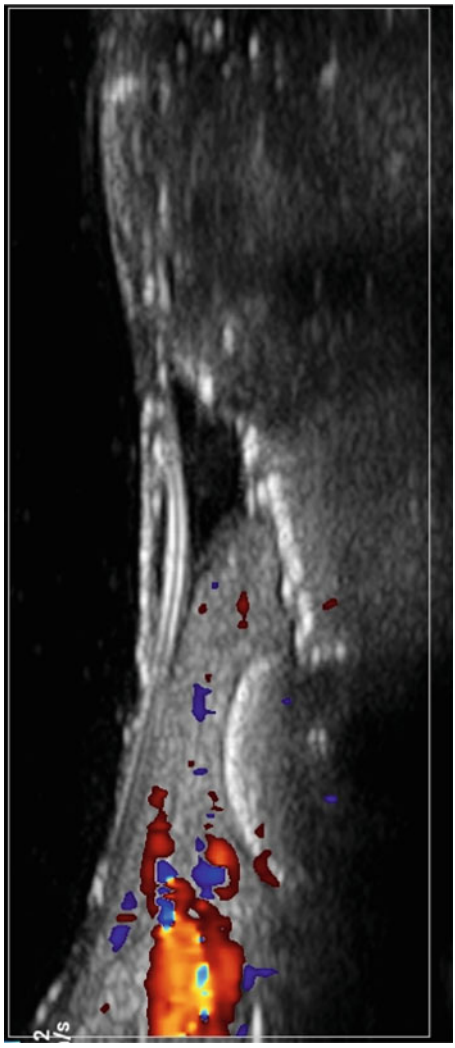

Fig. 7.8 B-mode image of the mental foramen with color flow indicating the mental artery and vein

stratifying the data, the differences in IAC readings were 0.1 mm, with high correlation (0.967). On the other hand, the correlations of maxillary sinus floor readings were weak ($r = 0.19$). Subsequently, a follow-up with larger sample size study was conducted by the same group [26]. The accuracy of ultrasound for identifying IAC was tested on ten patients with 18 implant osteotomies. The mean differences in residual bone height were 0.18 mm, with good correlation ($r = 0.61$). Therefore, this tested ultrasound device might be a useful alternative to locate IAC for implant surgeries in posterior mandible intraoperatively.

Bone boundaries should not be violated during implant surgery else, soft tissue damage and surgical complications may occur. Therefore, one study [25] aimed to

measure bone boundaries using a device that propagates 5 MHz ultrasonic waves through an aqueous milieu. Two parameters were measured: the depth of drill penetration into bone (drilled tract), and the distance between the drill tip to the bone boundary (residual depth). The correlations of ultrasound and mechanical measurements in the preclinical settings were ~0.99, with mean differences between 0.27 and 1.1 mm. In a clinical setting, the correlation between ultrasound and mechanical measurements was 0.78, with a mean difference of 0.05 mm. Radiographic and ultrasound measurements had correlations of 0.705 and 0.975 for the drilled tract and residual depth measures, respectively. The corresponding mean differences were 0.38 and 0.31 mm, respectively. Therefore, the study concluded this ultrasound method could be useful to monitor intraosseous drilling.

7.2.9 Conclusions

Ultrasound is versatile to identify clinically relevant anatomical structures during the treatment phase. It has been confirmed by clinical studies to accurately measure soft tissue phenotype and hard tissue morphotype, crestal ridge width and quality, mental foramen, greater palatine foramen, lingual nerve, lingual structures, etc. Therefore, ultrasound can already become an initial screening device at chairside for measuring ridge width and the other above mentioned anatomical landmarks during the treatment planning phase. During the surgery, it is fundamental to place an implant in an ideal position without disrupting vital structures in vicinity. Ultrasound can detect the impedance differences between the cancellous bone and the cortical bone that surrounds important structures; therefore, it has been shown to correctly identify IAN and maxillary sinus floor in lieu of radiographs to avoid surgical complications. Flapless implant surgery is becoming more popular because of tissue preservation, faster healing, and reduced morbidity. Cross-sectional drill-bit location could be imaged in real time with ultrasound to provide surgical feedback. There is no doubt ultrasound will be used in a conceivable future provided the device can be built more ergonomic, user friendly, more affordable, and more easily integrated into the current clinical workflow.

References

1. Branemark PI, et al. Osseointegrated implants in the treatment of the edentulous jaw experience from a 10-year period. Scand J Plast Reconstr Surg Suppl.1977;16:1–132. http://www.ncbi.nlm.nih.gov/pubmed/356184. ISSN: 0581-9474 (Print) 0581-9474 (Linking)
2. Lambrecht, JT et al. Long-term evaluation of submerged and nonsubmerged ITI solid-screw titanium implants: a 10-year life table analysis of 468 implants. Int J Oral Maxillofac Implants 2003;18 6:826–34. http://www.ncbi.nlm.nih.gov/pubmed/14696658. ISSN: 0882-2786 (Print) 0882-2786 (Linking).
3. Vandenberghe B, Jacobs R, Bosmans H. Modern dental imaging: a review of the current technology and clinical applications in dental practice. Eur Radiol. 2010;20 11:2637–55. https://doi.org/10.1007/s00330-010-1836-1. http://www.ncbi.nlm.nih.gov/pubmed/20544352. ISSN: 1432-1084 (Electronic) 0938-7994 (Linking).

4. Correa LR, et al. Planning of dental implant size with digital panoramic radiographs, CBCT-generated panoramic images, and CBCT cross-sectional images. Clin Oral Implants Res. 2014;25 6:690–5. https://doi.org/10.1111/clr.12126. ISSN: 1600-0501 (Electronic) 0905-7161 (Linking). http://www.ncbi.nlm.nih.gov/pubmed/23442085.
5. Chan HL, Misch K, Wang HL. Dental imaging in implant treatment planning. Implant Dent. 2010;19 4:288–98. https://doi.org/10.1097/ID.0b013e3181e59ebd. http://www.ncbi.nlm.nih.gov/pubmed/20683285. ISSN: 1538-2982 (Electronic) 1056-6163 (Linking)
6. Tyndall DA, et al. Position statement of the American academy of oral and maxillofacial radiology on selection criteria for the use of radiology in dental implantology with emphasis on cone beam computed tomography. Oral Surg Oral Med Oral Pathol Oral Radiol. 2012;113 6:817–26. https://doi.org/10.1016/j.oooo.2012.03.005. http://www.ncbi.nlm.nih.gov/pubmed/22668710. ISSN: 2212-4411 (Electronic)
7. Benavides E, et al. Use of cone beam computed tomography in implant dentistry: the international congress of oral implantologists consensus report. Implant Dent. 2012;21 2:78–86. https://doi.org/10.1097/ID.0b013e31824885b5. http://www.ncbi.nlm.nih.gov/pubmed/22382748. ISSN: 1538-2982 (Electronic) 1056-6163 (Linking).
8. Mandelaris GA, et al. American academy of periodontology best evidence consensus statement on selected oral applications for cone-beam computed tomography. J Periodontol. 2017;88 10:939–45. https://doi.org/10.1902/jop.2017.170234. http://www.ncbi.nlm.nih.gov/pubmed/28967333. ISSN: 1943-3670 (Electronic) 0022-3492 (Linking)
9. Bhaskar V, et al. Updates on ultrasound research in implant dentistry: a systematic review of potential clinical indications. Dentomaxillofac Radiol. 2018;47 6:20180076. https://doi.org/10.1259/dmfr.20180076. ISSN: 0250-832X (Print) 0250-832X (Linking). https://www.ncbi.nlm.nih.gov/pubmed/29791198.
10. Traxler M, et al. Ultrasonographic measurement of the soft-tissue of the upper jaw. Acta Radiol. 1991;32 1:3–5. http://www.ncbi.nlm.nih.gov/pubmed/2012725. ISSN: 0284-1851 (Print) 0284-1851 (Linking)
11. Culjat MO, et al. Ultrasound detection of submerged dental implants through soft tissue in a porcine model. J Prosthet Dent. 2008;99 3:218–24. https://doi.org/10.1016/S0022-3913(08)60046-3. http://www.ncbi.nlm.nih.gov/pubmed/18319093. ISSN: 0022-3913 (Print) 0022-3913 (Linking).
12. Culjat MO, et al. Ultrasound imaging of dental implants. Conf Proc IEEE Eng Med Biol Soc. 2012;2012:456–9. https://doi.org/10.1109/EMBC.2012.6345966. http://www.ncbi.nlm.nih.gov/pubmed/23365927. ISSN: 1557-170X (Print) 1557-170X (Linking)
13. De Bruyckere T, et al. Horizontal stability of connective tissue grafts at the buccal aspect of single implants: a 1-year prospective case series. J Clin Periodontol. 2015;42 9:876–82. https://doi.org/10.1111/jcpe.12448. http://www.ncbi.nlm.nih.gov/pubmed/26373422. ISSN: 1600-051X (Electronic) 0303-6979 (Linking).
14. Eghbali A, et al. Ultrasonic assessment of mucosal thickness around implants: validity reproducibility and stability of connective tissue grafts at the buccal aspect. Clin Implant Dent Relat Res. 2016;18 1:51–61.
15. Tattan M, et al. Ultrasonography for chairside evaluation of periodontal structures: a pilot study. J Periodontol. (2019). https://doi.org/10.1002/JPER.19.0342. ISSN: 1943-3670 (Electronic) 0022-3492 (Linking). https://www.ncbi.nlm.nih.gov/pubmed/31837020.
16. Traxler M, et al. Sonographic measurement versus mapping for determination of residual ridge width. J Prosthet Dent. 1992;67 3:358–61. http://www.ncbi.nlm.nih.gov/pubmed/1507101. ISSN: 0022-3913 (Print) 0022-3913 (Linking).
17. Bertram S, Emshoff R. Sonography of periimplant buccal bone defects in periodontitis patients: a pilot study. Oral Surg Oral Med Oral Pathol Oral Radiol Endod. 2008;105 1:99–103. https://doi.org/10.1016/j.tripleo.2007.01.014. https://www.ncbi.nlm.nih.gov/pubmed/17482844. ISSN: 1528-395X (Electronic) 1079-2104 (Linking).

18. Klein MO, et al. Ultrasound transmission velocity for noninvasive evaluation of jaw bone quality in vivo before dental implantation. Ultrasound Med Biol. 2008;34 12:1966–71. https://doi.org/10.1016/j.ultrasmedbio.2008.04.016. http://www.ncbi.nlm.nih.gov/pubmed/18620798. ISSN: 1879-291X (Electronic) 0301-5629 (Linking).
19. Kammerer PW, et al. Influence of a collagen membrane and recombinant platelet-derived growth factor on vertical bone augmentation in implantfixed deproteinized bovine bone–animal pilot study. Clin Oral Implants Res. 2013;24 11:1222–30. https://doi.org/10.1111/j.1600-0501.2012.02534.x. https://www.ncbi.nlm.nih.gov/pubmed/22762383. ISSN: 1600-0501 (Electronic) 0905-7161 (Linking)
20. Salmon B, Le Denmat D. Intraoral ultrasonography: development of a specific high-frequency probe and clinical pilot study. Clin Oral Investig. 2012;16 2:643–9. https://doi.org/10.1007/s00784-011-0533-z. https://www.ncbi.nlm.nih.gov/pubmed/21380502. ISSN: 1436-3771 (Electronic) 1432-6981 (Linking).
21. Degen K, et al. Assessment of cortical bone thickness using ultrasound. Clin Oral Implants Res. 2017;28 5:520–8. https://doi.org/10.1111/clr.12829. http://www.ncbi.nlm.nih.gov/pubmed/27018152. ISSN: 1600-0501 (Electronic) 0905-7161 (Linking).
22. Chan HL, et al. Non-invasive evaluation of facial crestal bone with ultrasonography. PLoS One. 2017;12 2:e0171237. https://doi.org/10.1371/journal.pone.0171237. http://www.ncbi.nlm.nih.gov/pubmed/28178323. ISSN: 1932-6203 (Electronic) 1932-6203 (Linking).
23. Lustig JP, et al. Ultrasound identification and quantitative measurement of blood supply to the anterior part of the mandible. Oral Surg Oral Med Oral Pathol Oral Radiol Endod. 2003;96 5:625–9. https://doi.org/10.1016/S107921040300516X. http://www.ncbi.nlm.nih.gov/pubmed/14600700. ISSN: 1079-2104 (Print) 1079-2104 (Linking).
24. Machtei EE, et al. Novel ultrasonic device to measure the distance from the bottom of the osteotome to various anatomic landmarks. J Periodontol. 2010;81 7:1051–5. https://doi.org/10.1902/jop2010.090621. http://www.ncbi.nlm.nih.gov/pubmed/20214439. ISSN: 1943-3670 (Electronic) 0022-3492 (Linking)
25. Rosenberg N, Craft A, Halevy-Politch J. Intraosseous monitoring and guiding by ultrasound: a feasibility study. Ultrasonics. 2014;54 2:710–9. https://doi.org/10.1016/j.ultras2013.09008. http://www.ncbi.nlm.nih.gov/pubmed/24112599. ISSN: 1874-9968 (Electronic) 0041-624X (Linking).
26. Zigdon-Giladi H, et al. Intraoperative measurement of the distance from the bottom of osteotomy to the mandibular canal using a novel ultrasonic device. Clin Implant Dent Relat Res. 2016;18 5:1034–1041. https://doi.org/10.1111/cid.12362. http://www.ncbi.nlm.nih.gov/pubmed/26134492. ISSN: 1708-8208 (Electronic) 1523-0899 (Linking).
27. Chan HL, et al. Non-invasive evaluation of facial crestal bone with ultrasonography. PLoS One 2017;12 e0171237.
28. Barootchi S, et al. Ultrasonographic characterization of lingual structures pertinent to oral, periodontal, and implant surgery. Clin Oral Implants Res. (2020). https://doi.org/10.1111/clr.13573. https://www.ncbi.nlm.nih.gov/pubmed/31925829. ISSN: 1600-0501 (Electronic) 0905-7161 (Linking).
29. Veltri M, et al. The speed of sound correlates with implant insertion torque in rabbit bone: an in vitro experiment. Clin Oral Implants Res. 2010;21 7:751–5. https://doi.org/10.1111/j1600-0501.2009.01873.x. https://www.ncbi.nlm.nih.gov/pubmed/20384706. ISSN: 1600-0501 (Electronic) 0905-7161 (Linking).
30. Kumar VV, et al. Relation between bone quality values from ultrasound transmission velocity and implant stability parameters–an ex vivo study. Clin Oral Implants Res. 2012;23 8:975–80. https://doi.org/10.1111/j.1600-0501.2011.02250.x. https://www.ncbi.nlm.nih.gov/pubmed/22092939. ISSN: 1600-0501 (Elec- tronic) 0905-7161 (Linking).

31. Ossi Z, et al. In vitro assessment of bone-implant interface using an acoustic emission transmission test. Proc Inst Mech Eng H. 2012;226 1:63–9. https://doi.org/10.1177/0954411911428696. https://www.ncbi.nlm.nih.gov/pubmed/22888586. ISSN: 0954-4119 (Print) 0954-4119 (Linking).
32. Ossi Z, et al. Transmission of acoustic emission in bones, implants and dental materials. Proc Inst Mech Eng H. 2013;227 11:1237–45. https://doi.org/10.1177/0954411913500204. https://www.ncbi.nlm.nih.gov/pubmed/23963748. ISSN: 2041-3033 (Electronic) 0954-4119 (Linking).
33. Mathieu V, et al. Numerical simulation of ultrasonic wave propagation for the evaluation of dental implant biomechanical stability. J Acoust Soc Am. 2011;129 6:4062–72. https://doi.org/10.1121/13586788. https://www.ncbi.nlm.nih.gov/pubmed/21682427. ISSN: 1520-8524 (Electronic) 0001-4966 (Linking).
34. Mathieu V, et al. Ultrasonic evaluation of dental implant biomechanical stability: an in vitro study. Ultrasound Med Biol. 2011;37 2:262–70. https://doi.org/10.1016/j.ultrasmedbio.2010.10.008. https://www.ncbi.nlm.nih.gov/pubmed/21257090. ISSN: 1879-291X (Electronic) 0301-5629 (Linking).
35. Mathieu V, et al. Biomechanical determinants of the stability of dental implants: influence of the bone-implant interface properties. J Biomech. 2014;47 1:3–13. https://doi.org/10.1016/j.jbiomech.2013.09.021. https://www.ncbi.nlm.nih.gov/pubmed/24268798. ISSN: 1873-2380 (Electronic) 0021-9290 (Linking).
36. Vayron R, et al. Assessment of in vitro dental implant primary stability using an ultrasonic method. Ultrasound Med Biol. 2014;40 12:2885–94. https://doi.org/10.1016/j.ultrasmedbio.2014.03.035. https://www.ncbi.nlm.nih.gov/pubmed/25308939. ISSN: 1879-291X (Electronic) 0301-5629 (Linking).
37. Mathieu V, et al. Biomechanical determinants of the stability of dental implants: influence of the bone-implant interface properties. J Biomech. 2014;47 1:3–13. https://doi.org/10.1016/j.jbiomech.2013.09.021. https://www.ncbi.nlm.nih.gov/pubmed/24268798. ISSN: 1873-2380 (Electronic) 0021-9290 (Linking).
38. Vayron R, et al. Finite element simulation of ultrasonic wave propagation in a dental implant for biomechanical stability assessment. Biomech Model Mechanobiol. 2015;14 5:1021–32. https://doi.org/10.1007/s10237-015-0651-7. https://www.ncbi.nlm.nih.gov/pubmed/25619479. ISSN: 1617-7940 (Elec- tronic) 1617-7940 (Linking).
39. Vayron R, et al. Assessment of the biomechanical stability of a dental implant with quantitative ultrasound: a three-dimensional finite element study. J Acoust Soc Am. 2016;139 2:773–80. https://doi.org/10.1121/1.4941452. https://www.ncbi.nlm.nih.gov/pubmed/26936559. ISSN: 1520-8524 (Electronic) 0001-4966 (Linking).
40. Kemmerer JP, et al. Assessment of high-intensity focused ultrasound treatment of rodent mammary tumors using ultrasound backscatter coefficients. J Acoust Soc Am. 2013;134 2:1559–68. https://doi.org/10.1121/1.4812877. http://www.ncbi.nlm.nih.gov/pubmed/23927196. ISSN: 1520-8524 (Electronic) 0001-4966 (Linking).
41. Fu JH, et al. The accuracy of identifying the greater palatine neurovascular bundle: a cadaver study. J Periodontol. 2011;82 7:1000–6. https://doi.org/10.1902/jop.2011.100619. https://www.ncbi.nlm.nih.gov/pubmed/21284546. ISSN: 1943-3670 (Electronic) 0022-3492 (Linking).
42. Methathrathip D, et al. Anatomy of greater palatine foramen and canal and pterygopalatine fossa in Thais: considerations for maxillary nerve block. Surg Radiol Anat. 2005;27 6, 511–6. https://doi.org/10.1007/s00276-005-0016-5. https://www.ncbi.nlm.nih.gov/pubmed/16228112. ISSN: 0930-1038 (Print) 0930-1038 (Linking).
43. Behnia H, Kheradvar A, Shahrokhi M. An anatomic study of the lingual nerve in the third molar region. J Oral Maxillofacial Surg. 2000;58 6:649–51. Discussion 652. http://sfx.lib.umich.edu:9003/sfx_local?sid=Entrez%3APubMed;id=pmid%3A10847287. ISSN: 0278-2391.
44. Pogrel MA, Goldman K, Lingual flap retraction for third molar removal. J Oral Maxillofacial Surg. 2004;62 9:1125–30. ISSN: 0278-2391. http://sfx.lib.umich.edu:9003/sfx_local?sid=Entrez%3APubMed;id=pmid%3A15346365.

45. Chan HL, et al. The significance of the lingual nerve during periodontal/implant surgery. J Periodontol. 2010;81 3:372–7. https://doi.org/10.1902/jop.2009.090506. http://www.ncbi.nlm.nih.gov/pubmed/20192863. ISSN: 1943-3670 (Electronic) 00223492 (Linking).
46. Bataineh AB. Sensory nerve impairment following mandibular third molar surgery. J Oral Maxillofac Surg. 2001;59 9:1012–7. discussion 1017. https://doi.org/S0278-2391(01)58639-5[pii]10.1053/joms.2001.25827. http://www.ncbi.nlm.nih.gov/entrez/query.fcgi?cmd=Retrieve&db=PubMed&dopt=Citation&list_uids=11526568. ISSN: 0278-2391 (Print).
47. Gomes AC, et al. Lingual nerve damage after mandibular third molar surgery: a randomized clinical trial. J Oral Maxillofac Surg. 2005;63 10:1443–6. https://doi.org/S0278-2391(05)01033-5[pii]10.1016/j.joms.2005.06.012. http://www.ncbi.nlm.nih.gov/entrez/query.fcgi?cmd=Retrieve&db=PubMed&dopt=Citation&list_uids=16182911. ISSN: 0278-2391 (Print).
48. Gulicher D, Gerlach KL. Sensory impairment of the lingual and inferior alveolar nerves following removal of impacted mandibular third molars. Int J Oral Maxillofac Surg. 2001;30 4:306–12. https://doi.org/S0901-5027(01)90057-8[pii]10.1054/ijom.2001.0057. http://www.ncbi.nlm.nih.gov/entrez/query.fcgi?cmd=Retrieve&db=PubMed&dopt=Citation&list_uids=11518353. ISSN: 0901-5027 (Print).
49. Hillerup S, Stoltze K. Lingual nerve injury in third molar surgery I. Observations on recovery of sensation with spontaneous healing. Int J Oral Maxillofac Surg. 2007;36 10:884–9. https://doi.org/S0901-5027(07)00231-7[pii]10.1016/j.ijom.2007.06.004. http://www.ncbi.nlm.nih.gov/entrez/query.fcgi?cmd=Retrieve&db=PubMed&dopt=Citation&list_uids=17766086. ISSN: 0901-5027 (Print).
50. Valmaseda-Castellon E, Berini-Aytes L, Gay-Escoda C. Lingual nerve damage after third lower molar surgical extraction. Oral Surg Oral Med Oral Pathol Oral Radiol Endod. 2000;90 5:567–73. https://doi.org/S1079-2104(00)56151-4[pii]10.1067/moe-2000.110034. http://www.ncbi.nlm.nih.gov/entrez/query.fcgi?cmd=Retrieve&db=PubMed&dopt=Citation&list_uids=11077378. ISSN: 1079-2104 (Print).
51. Askar H, et al. Morphometric analysis of the mental foramina, accessory mental foramina, and anterior loops: a CBCT study. Acta Sci Dental Sci. 2018;2 12:126–32.
52. Bartling R, Freeman K, Kraut RA. The incidence of altered sensation of the mental nerve after mandibular implant placement. J Oral Maxillofac Surg. 1999;57 12:1408–12. https://doi.org/10.1016/s0278-2391(99)90720-6. https://www.ncbi.nlm.nih.gov/pubmed/10596660. ISSN: 0278-2391 (Print) 0278-2391 (Linking).
53. Walton JN. Altered sensation associated with implants in the anterior mandible: a prospective study. J Prosthet Dent. 2000;83 4:443–9. https://doi.org/10.1016/s0022-3913(0)70039-4. https://www.ncbi.nlm.nih.gov/pubmed/10756294. ISSN: 0022-3913 (Print) 0022-3913 (Linking).
54. Wismeijer D, et al. Patients' perception of sensory disturbances of the mental nerve before and after implant surgery: a prospective study of 110 patients. Br J Oral Maxillofac Surg. 1997;35 4:254–9. https://doi.org/10.1016/s0266-4356(97)90043-7. https://www.ncbi.nlm.nih.gov/pubmed/9291263. ISSN: 0266-4356 (Print) 0266-4356 (Linking).